SOUTHERN BRAZILIAN JOURNAL OF CHEMISTRY

$(Cu_{0.4}Al_{0.3})TaSe_2$: PREPARATION AND CRYSTAL STRUCTURE ANALYSIS FROM X-RAY POWDER DIFFRACTION

GRIMA-GALLARDO, Pedro[1,2,3]; DURÁN, Sonia[4]; MUÑOZ, Marcos[4], RAI, Dibya P.[5], DELGADO, Gerzon E.[6*]

[1] Centro de Estudios en Semiconductores (CES). Departamento de Física, Facultad de Ciencias, Universidad de Los Andes, Mérida, Venezuela

[2] Centro Nacional de Tecnologías Ópticas (CNTO), Mérida, Venezuela

[3] Centro de Investigaciones de Astronomía (CIDA), Mérida, Venezuela

[4] Universidad Centro-Occidental "Lisandro Alvarado", Barquisimeto, Venezuela

[5] Physical Sciences Research Center (PSRC), Department of Physics, Pachhunga University College, Aizawl, Mizoram, India

[8] Laboratorio de Cristalografía, Departamento de Química. Facultad de Ciencias, Universidad de Los Andes. Mérida, Venezuela

** Correspondence author*
e-mail: gerzon@ula.ve

Received 01 June 2020; received in revised form 30 August 2020; accepted 07 September 2020

ABSTRACT

A new phase of the $(CuAlSe_2)_{1-x}(TaSe)_x$ alloy system was synthesized by the melt and annealing technique and studied by SEM, DTA, and XRPD techniques. Its structure has been refined by the Rietveld method using X-ray powder diffraction data. The new alloy corresponds with the stoichiometry $Cu_{0.4}Al_{0.3}TaSe_2$. This compound crystallizes in the hexagonal space group $P\bar{6}m2$ (Nº 187) with a MoS_2-type structure, and unit cell parameters *a* = 3.455(2) Å, *c* = 13.423(4) Å, V = 138.7(1) Å^3, Z =2. The crystal structure is based on the MoS_2-type of stacking of $TaSe_2$ layers with a partial ordering of Cu and Al cations over the tetrahedral sites. The powder pattern was composed of 63.1% of the principal phase $Cu_{0.4}Al_{0.3}TaSe_2$ and 29.9% of $CuAlSe_2$, 7.0% of $TaSe_3$, as the secondary phases

Keywords: Alloys, X-ray diffraction, crystal structure, MoS_2 type

1. INTRODUCTION

The compounds with ternary structures of the chalcopyrite family Cu-III-VI_2 (III = Al, Ga, In, VI = S, Se, Te) form a wide group of semiconductor materials with diverse optical and electrical properties (Shay and Wernik, 1974). They crystallize with tetragonal symmetry, and the addition of an II-VI (II = Mn, Fe, Co, Ni, Ta) binary compound produces alloys of the type $(Cu\text{-}III\text{-}VI_2)_{1-x}(II\text{-}VI)_x$ (Parthé, 1995). The formation of some member with compositions $Cu_2\text{-}II\text{-}III\text{-}Se_5$ (x = ⅓), $Cu\text{-}II\text{-}III\text{-}Se_3$ (x = ½), $Cu\text{-}II_2\text{-}III\text{-}Se_4$ (x =⅔) have been reported (Grima-Gallardo *et al*., 2000; 2001a; 2001b; Mora *et al*., 2007; Delgado *et a*l., 2008; 2019). All these phases fulfill the rules of formation of adamantane compounds and belong to the normal semiconductor compound families derivatives of the II-VI binary semiconductors (Parthé, 1995).

These type of semiconductors combined with magnetic behavior give place to the so-called "diluted magnetic semiconductors" or "semi-magnetic semiconductors", which have been largely investigated in the last years due to their possible application in spintronic devices (Jain, 1991; Pearton *et al*., 2003). Besides, chalcogen-based (VI = S, Se, Te) begin to be studied as potential trainers of "wide bandgap

semiconductors", which are essential for electronic devices and energy applications because of their high optical transparency, controllable carrier concentration, and tunable electrical conductivity (Woods-Robinson *et al*., 2020). On the other hand, Ta-based chalcogenides are usually used to form alloys with applicable properties due to their high melting point (Kikkawa *et al., 1982;* Hayashi *et al.,* 2007; Ali *et al*., 2015*).*

In this work, and as part of ongoing structural studies on semiconductors of the system $(Cu\text{-}III\text{-}VI_2)_{1-x}(Ta\text{-}VI)_x$ (Grima-Gallardo *et al*., 2007; 2008; 2018a; 2018b; Delgado *et a*l., 2007; 2008), we report the synthesis and structural analysis of the quaternary semiconductor with composition $Cu_{0.4}Al_{0.3}TaSe_2$. This compound is a new member of the $(CuAlSe_2)_{1-x}(TaSe)_x$ family, which is a related phase of the hexagonal compound 2H-$Cu_{0.52}TaSe_2$ *(*Ali *et al*., 2015*).*

2. MATERIALS AND METHODS

2.1. Preparation

Starting materials (Cu, Al, Ta, and Se) with nominal purity of 99.99 wt. % (Goodfellow) in the stoichiometric ratio were mixed in an evacuated (10^{-4} Torr) and sealed quartz tube with the inner walls previously carbonized to prevent the chemical reaction of the elements with quartz. The quartz ampoule is heated until 493 K (melting point of Se), keeping this temperature for 48 h and shaking all the time using an electromechanical motor. This procedure guarantees the formation of binary species at low temperatures avoiding the existence of Se free gas at high temperature, which could produce explosions or Se deficiency in the ingot. Then the temperature was slowly increased until 1423 K, with the mechanical shaker always connected for better mixing of the components. After 24 h, the cooling cycle begins until the anneal temperature (800K) with the mechanical shaker is disconnected. The ampoule is keeping at the annealing temperature for 1 month to ensure the thermal equilibrium. Then the furnace is switching off.

2.2. Scanning Electron Microscopy

Stoichiometric relations of the sample were investigated by scanning electron microscopy (SEM) technique, using a Hitachi S2500 equipment. The microchemical composition was found by an energy-dispersive x-ray spectrometer (EDS) coupled with a computer-based multichannel analyzer (MCA, Delta III analysis, and Quantex software, Kevex). For the EDS analysis, Kα lines were used. The accelerating voltage was 15 kV. The samples were tilted 35 degrees. A standardless EDS analysis was made with a relative error of $\pm$ 5-10% and detection limits of the order of 0.3 wt %, where the k-ratios are based on theoretical standards.

2.3. Differential Thermal Analysis

Differential Thermal Analysis (DTA) measurements were carried out in a fully automatic Perkin-Elmer apparatus, which consists of a Khantal resistance furnace (T_{max} = 1650 K) equipped with Pt/Pt-Rh thermocouples and an informatics system for the automatic acquisition data. The internal standard used was a high purity (99.99 wt. %) piece of gold. The temperature runs have been performed from ambient temperature to 1400-1500 K, which is the recommended operative limit. The heating rate was controlled electronically to 20 Kh-1; the cooling rate was given by the natural cooling of the furnace after switching off. From the thermogram, transition temperatures were manually obtained from the ΔT vs. T graph with the criteria that the transition occurs at the intersection of the baseline with the slope of the thermal transition peak, as usual. The maximum error committed in the determination of transition temperatures by this method was estimated to be $\pm$ 10 K.

2.4. X-Ray Powder Diffraction

X-ray powder diffraction data were collected employing a diffractometer (Siemens D5005) equipped with a graphite monochromator (CuKα, λ = 1.54059 Å) at 40 kV and 20 mA. Quartz was used as an external standard. The sample was scanned from 5-100° 2θ, with a step size of 0.02° and counting time of 20 s. The peak positions were extracted utilizing single-peak profile fitting carried out through the Bruker Diffracplus software. For the Rietveld refinement, the whole diffraction data was used.

3. RESULTS AND DISCUSSION:

Three different regions of the ingot were scanned, and the average atomic percentages from SEM are summarized in Table 1.

Table 1. *SEM experimental results for* $(CuAlSe_2)_{1-x}(TaSe)_x$ *alloy system for x = ½*

Nominal stoichiometry (%)	Experimental stoichiometry (%)
Cu=16.67	Cu = 09.8 ± 0.3
Al=16.67	Al = 07.0 ± 0.5
Ta=16.67	Ta = 29.8 ± 0.4
Se=50.00	Se = 53.4 ± 0.6

The mean experimental stoichiometry observed has been calculated as $Cu_{0.4}Al_{0.3}TaSe_2$. In Figure 1, the microphotography of this phase is shown. It can be observed the platelets that confirms the laminar character of the crystal structure for this phase.

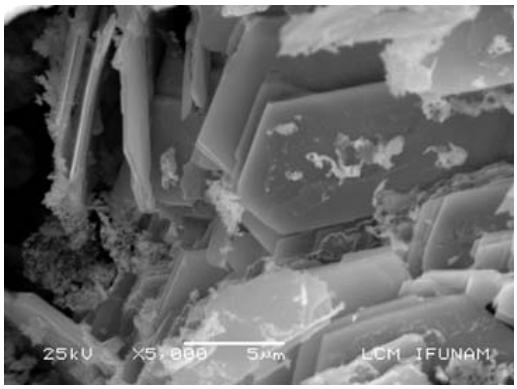

Figure 1*. Microphotography of the hexagonal* $(CuAlSe_2)_{1-x}(TaSe)_x$ *alloy system for x = ½*

In Figure 2, DTA heating and cooling cycles for $(CuAlSe_2)_{1-x}(TaSe)_x$ x= ½ alloy are plotted. In the heating cycle, the sample shows a peritectic melting point with a relatively wide solid+liquid region. The differential thermal analysis (DTA) indicates that this compound melts at 1445 K.

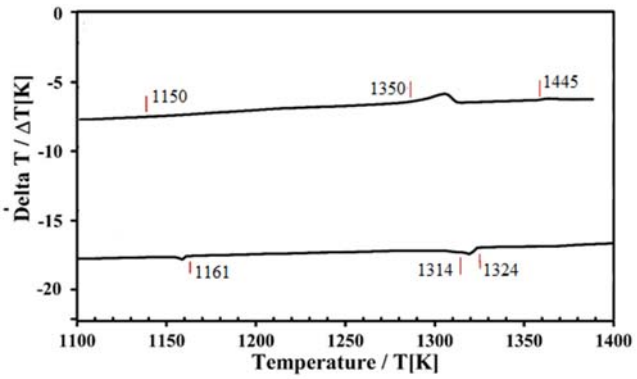

Figure 2*. DTA heating (top) and cooling (bottom) cycles for* $(CuAlSe_2)_{1-x}(TaSe)_x$ *alloys with x = ½*

Figure 3 shows the resulting X-ray powder diffractogram. An automatic search in the PDF-ICDD database (ICDD, 2013) indicates that the powder pattern also contains small amounts of the ternary $CuAlSe_2$ (PDF 01-075-0101) and the binary $TaSe_3$ (PDF 00-18-1310). Bragg positions of the diffraction lines from these phases are also indicated in Figure 3. The remaining intense peaks corresponding to the phase of interest were indexed in a hexagonal cell with: *a* = 3.454 Å and *c* = 13.411 Å, using the program Dicvol04 (Boultif and Louër, 2004). A revision of the diffraction lines of the main phase taking into account the sample composition and unit cell parameters suggested that this material is isostructural with the phase 2H-$Cu_{0.52}TaSe_2$, recently reported, which crystallize in the space group $P\bar{6}m2$ (Nº 187) (Ali *et al*., 2015).

Structural refinement was performed with the Rietveld method (Rietveld, 1969) using the program Fullprof Suite (Rodríguez-Carvajal, 1993) by applying a Cox-Hastings pseudo-Voigt function (Thompson *et al*., 1987). The background was fitted using a linear interpolation between a set of background points with refinable heights. The angular dependence of the peak full width at half maximum (FWHM) was described by the Caglioti's formula (Caglioti *et al*., 1958). The thermal motion of the atoms was described by one overall isotropic temperature factor for each phase.

The atomic coordinates of $Cu_{0.52}TaSe_2$ (Ali *et al*., 2015) were used as a starting model for the quaternary (CuAl)x$TaSe_2$, where the occupation factors of Cu and Al atoms were refined. The atomic positions of the ternary $CuAlSe_2$ (Hahn *et al*., 1953) and the binary $TaSe_3$ (Bjerkelund and Kjekshus, 1965) were included as secondary phases in the refinement.

The results of the Rietveld refinement are summarized in Table 2. The final Rietveld refinement converged to the following weight fraction percentages: $Cu_{0.4}Al_{0.3}TaSe_2$ (63.1%), $CuAlSe_2$ (29.9%) and $TaSe_3$ (7.0%).

It should be noted that the occupancy factors for Cu and Al cations are in good agreement with the values found in chemical analysis (see Table 3), and the stoichiometry of this alloy is: $Cu_{0.4}Al_{0.3}TaSe_2$.

Figure 3 shows the observed, calculated, and different profiles for the final cycle of Rietveld refinement. Atomic coordinates and isotropic temperature factor for the new phase $Cu_{0.4}Al_{0.3}TaSe_2$ are shown in Table 3.

Table 2. *Rietveld refinement results for* $Cu_{0.4}Al_{0.3}TaSe_2$

Molecular formula	$Cu_{0.4}Al_{0.3}TaSe_2$
Molecular weight (g/mol)	373.56
System	hexagonal
Space group	$P\bar{6}m2$ (187)
D_{calc} (g/cm^{-3})	2.22
a (Å)	3.455(2)
c (Å)	13.423(4)
V (Å^3)	138.7(1)
Z	2
R_{exp} (%)	7.8
R_p (%)	8.8
R_{wp} (%)	9.1
S	1.2
R_B (%)	8.5

$R_p = 100\ \sum|y_{obs} - y_{calc}| / \sum|y_{obs}|$ $S = [R_{wp} / R_{exp}]$
$R_{exp} = 100[(N+C)/\sum_w(y_{obs}^2)]^{1/2}$ $R_B = 100\ \sum_k|I_k - Ic_k| / \sum_k |I_k|$
$R_{wp} = 100\ [\sum_w|y_{obs} - y_{calc}|^2 / \sum_w|y_{obs}|^2]^{1/2}$
N-P+C= degrees of freedom

The crystal structure is based on the MoS_2 type of stacking of $TaSe_2$ layers with a partial ordering of Cu and Al cations over the tetrahedral sites. Figure 4 shown the tetrahedral around the Cu An Al cations with the $TaSe_2$ layer at the center.

$Cu_{0.4}Al_{0.3}TaSe_2$ is a new chalcogenide compound related to the layered 2H-$Cu_{0.52}TaSe_2$ phase, with potential use as a wide bandgap semiconductor (Woods-Robinson *et al*., 2020).

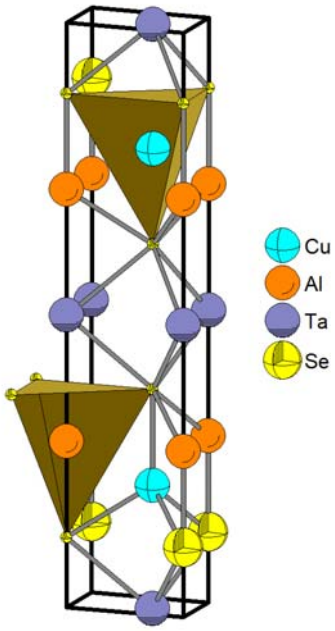

Figure 4. *Unit cell representation for* $Cu_{0.4}Al_{0.3}TaSe_2$*, showing the tetrahedral around the Cu and Al cations*

4. CONCLUSIONS:

The phase with x = ½ for the alloy system $(CuAlSe_2)_{1-x}(TaSe)_x$ has been synthesized and studied by SEM, DTA, and XRPD techniques. A new phase with experimental stoichiometry $Cu_{0.4}Al_{0.4}TaSe_2$ was identified and refined. This alloy crystallizes in the hexagonal structure, space group $P\bar{6}m2$ (N° 187), with unit cell parameters *a* = 3.455(2) Å, *c* = 13.423(4) Å, V = 138.7(1) Å^3. The powder pattern was composed of 63.1% of the principal phase $Cu_{0.4}Al_{0.3}TaSe_2$ and 29.9% of $CuAlSe_2$, 7.0% of $TaSe_3$, as the secondary phases.

5. ACKNOWLEDGMENTS

This work was supported by FONACIT (Grant LAB-97000821).

6. REFERENCES:

1. Ali, S.I., Mondal, S., van Smaalen, S. *Z. Anorg. Allg. Chem*. **2015**, 641, 464.
2. Bjerkelund, E., Kjekshus, A. *Acta Chem. Scand.* **1965**, 19, 701.
3. Boultif, A., Louër, D. *J. App. Cryst*. **2004**, 37, 724.
4. Cagliotti, G., Paoletti, A., Ricci, F.P. *Nucl. Instrum*. **1958**, 3, 223.
5. Delgado, G.E., Delgado-Niño, P., Grima-Gallardo, P. *Tchê Quím. J*. **2019**, 16, 848.
6. Delgado, G.E., Mora, A.J., Grima-Gallardo, P., Durán, S., Muñoz, M., Quintero, M. *Cryst. Res. Technol*. **2008**b, 43, 783.
7. Delgado, G.E., Mora, A.J., Grima-Gallardo, P., Muñoz, M., Durán, S., Quintero, M. *Physica B*, **2008**, 403, 3228.
8. Delgado, G.E., Mora, A.J., Grima-Gallardo, P., Quintero, M. *J. Alloys Comp*. **2008**a, 454, 306.
9. Grima-Gallardo, P., Cárdenas, K., Quintero, M., Ruiz, J., Delgado, G.E. *Mater. Res. Bull*. **2001**, 36, 861.
10. Grima-Gallardo, P., Méndez, L., Delgado, G.E., Cabrera, H., Pérez-Cappé, E., Zumeta-Dubé, I., Rodríguez, A., Aitken, J.A., Rai, D.P. *Int. J. Exp. Spectroscopic. Tech.* **2018**, 3, 16.
11. Grima-Gallardo, P., Molina, L., Quintero, M., Tovar, R., Ruiz, J., Quintero, E., Delgado, G.E., Maury, L. *phys. stat. sol. (b)*, **2000**, 220, 377.
12. Grima-Gallardo, P., Muñoz, M., Delgado,

G.E., Briceño, J.M., Ruiz, J. *phys. stat. sol. (b)*, **2001**, 241, 1789.
13. Grima-Gallardo, P., Muñoz, M., Durán, S., Delgado, G.E., Quintero, M., Ruiz, J. *Mater. Res. Bull*. **2007**, 42, 2067.
14. Grima-Gallardo, P., Muñoz, M., Durán, S., Quintero, E., Quintero, M., Morocoima, M., Calderón, E., Delgado, G.E., Romero, H. *Phys. Stat. Sol. (a*), **2008**, 205, 1552.
15. Grima-Gallardo, P., Ruiz, J. Phys. Stat. Sol. (a) 173 (1999) 283-288.
16. Grima-Gallardo,P., Izarra, O., L. Méndez, L., Torres, S., Quintero, M., Cabrera, H., Pérez-Cappé, E., Zumeta-Dubé, I., Rodríguez, A., Aitken, J.A., Rai, D.P. *J. Alloys Compd*. **2018**, 747, 176.
17. Hahn, H., Meyer, A.D., Frank, G., Klingler, W., Stoerger, G. *Z. Anorg. Allg. Chem*, **1953**, 271, 153.
18. Hayashi, K., Tanico, Y., Kawachi, K., Nakata, Y., Inoue, K., Maeda, N. *J. Alloys Compd*. **2007**, 442, 117.
19. *International Centre for Diffraction Data* (ICDD), *Powder Diffraction File (Set 1-65).* Newtown Square, PA, USA, **2013**.
20. Jain, M. *Diluted Magnetic Semiconductors*. World Scientific, Singapore, **1991**.
21. Kikkawa, S., Shinya, K., Koizumi, M. *J. Solid Stat. Chem*. **1982**, 41, 323.
22. Mora, A.J., Delgado, G.E., Grima-Gallardo, P., Quintero M. *Phys. Stat. Sol. (a)*. **2007**, 204, 547.
23. Parthé E. *Wurtzite and Sphalerite Structures*. In: J.H. Westbrook, R.L. Fleischer (eds), *Intermetallic Compounds, Principles, and Applications*. Vol. 1, John Wiley & Sons, Chichester, UK, **1995**.
24. Pearton, S.J., Abernathy, C.R., Norton, D.P., Hebard, A.F., Park, Y.D., Boatner, L.A., Budai, J.D. *Mater. Sci. Eng.* **2003**, R40, 137.
25. Rietveld, H.M. *J. App. Cryst*. **1969**, 2, 65.
26. Rodriguez-Carvajal, J. *Phys. B: Cond. Matter*, **1993**, 192, 55.
27. Shay J.L., Wernik J.H. *Ternary chalcopyrite semiconductors: Growth, electronic properties and applications*, Pergamon Press., Oxford, **1974**.
28. Thompson, P., Cox, D.E., Hastings, J.B. *J. App. Cryst*. **1987**, 20, 79.
29. Woods-Robinson, R., Yanbing Han, Y., Zhang, H., Ablekim, T., Khan, K., Persson, K., Zakutayev, A. *Chem. Rev*., **2020**, 120, 4007.

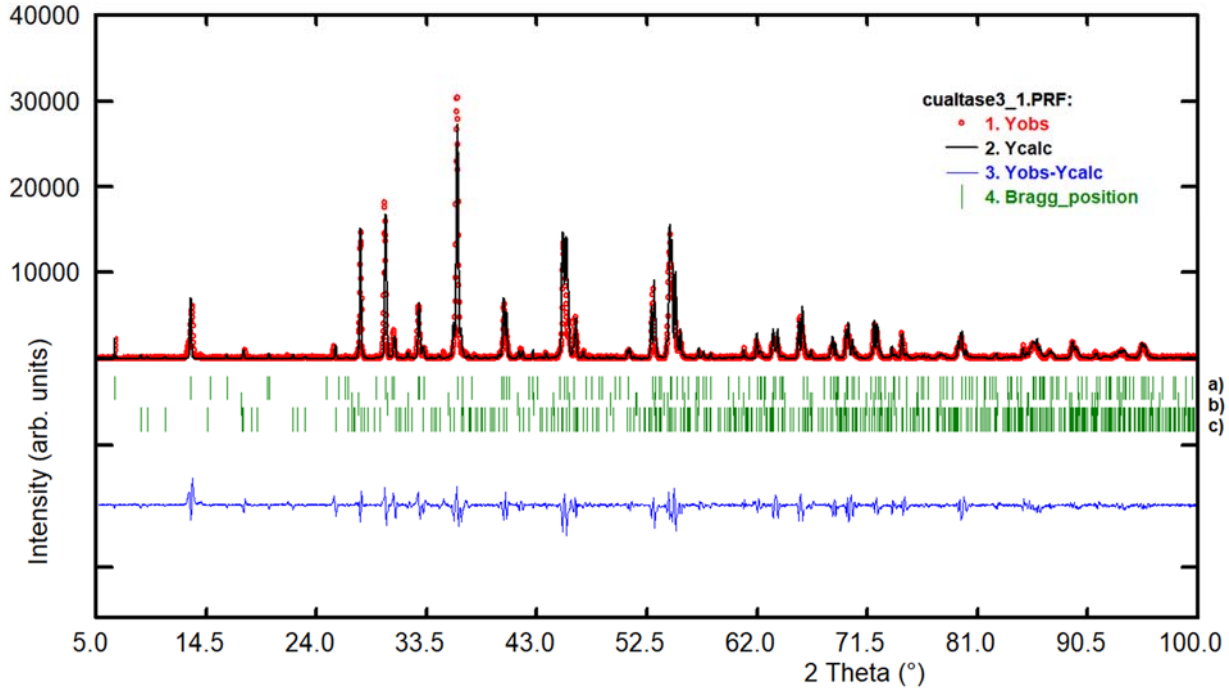

Figure 3. *Rietveld refinement of the powder pattern shown the new phase a) $Cu_{0.4}Al_{0.3}TaSe_2$, together with the secondary phases b) $CuAlSe_2$ and c) $TaSe_3$. The lower trace is the difference curve between observed and calculated patterns. The Bragg reflections are indicated by vertical bars*

Table 3. *Atomic coordinates (Å) and isotropic temperature factors for $Cu_{0.4}Al_{0.3}TaSe_2$, derived from the Rietveld refinement.*

Atom	Ox.	Site	*x*	*y*	*z*	foc	B (Å^2)
Cu	+1	*2i*	*⅔*	*⅓*	*0.2124(8)*	0.41(2)	0.6(4)
Al	+3	*2g*	0	0	0.2845(7)	0.32(2)	0.6(4)
Ta1	+2	*1b*	0	0	½	1	0.6(4)
Ta2	+2	*1e*	*⅔*	*⅓*	*0*	1	0.6(4)
Se1	-2	*2i*	*⅔*	*⅓*	*0.3762(7)*	1	0.6(4)
Se2	-2	*2g*	0	0	0.1205(7)	1	0.6(4)

The SOUTHERN BRAZILIAN JOURNAL OF CHEMISTRY (ISSN: 2674-6891; 0104-5431) is an open-access journal since 1993. Journal DOI: 10.48141/SBJCHEM. http://www.sbjchem.com. This text was introduced in this file in 2021 for compliance reasons.